PHYSICAL REVIEW B VOLUME 27, NUMBER 2 15 JANUARY 1983

Random T-matrix approach to one-dimensional localization

C. J. Lambert and M. F. Thorpe
Department of Physics and Astronomy, Michigan State University, East Lansing, Michigan 48824
(Received 29 July 1982)

We develop simple quantitative formulas for the inverse localization length of a one-dimensional sequence of scatterers that are valid in the strong and in the weak scattering limits. These formulas are shown to agree with numerical results obtained for chains with up to 10^6 scatterers. We discuss the special circumstances under which a recent random-phase result becomes quantitatively correct.

I. INTRODUCTION

The effect of disorder on the transport properties of noncrystalline materials has long been a subject of considerable interest.[1-12] Recognition of the importance of localization has led to many calculations of inverse localization lengths, but there exist surprisingly few exact results. As a consequence of this and in view of recent experiments[2] on low-dimensional systems, much attention has been directed towards disordered systems described by a one-dimensional (1D) random potential.

A variety of techniques are available for determining the inverse localization length α of an infinitely long 1D wire (for a recent review see Erdös and Henderson[3]). These range from numerical algorithms[4,5] to theories which determine the probability distribution of α.[6,7] However, many of these techniques are most suited to particular systems; a general prescription for extracting the inverse localization length from a given Hamiltonian does not exist. The aim of this paper is to discuss a simple approach to this problem which is applicable to a wide range of 1D random systems.

The method is based on a random transfer matrix approach which was employed recently[8-11] to examine the statistical properties of the inverse localization length. In essence, the resistance of a 1D wire is calculated by breaking it into a series of segments. If ρ_i is the dimensionless resistance of the ith segment, it can be shown (a complete discussion is given in Sec. II) that

$$\alpha=\alpha_1+\alpha_2 , \tag{1}$$

where

$$\alpha_1=\langle \ln(1+\rho)\rangle \tag{2}$$

with the angular brackets denoting an average over all segments.

In applications mentioned above,[8,9] α_2 is eliminated by introducing a random-phase assumption. This assumption is not generally valid.[12] However, it can be shown analytically for large ρ_i (Ref. 12) and numerically for small ρ_i that by choosing long enough segments, α_2 can be made negligibly small[13] compared with α_1. In view of this, the *qualitative* results obtained from the random-phase assumption, which do not depend on a detailed knowledge of the ρ_i, are expected to apply to a wide variety of 1D systems. In what follows we consider the possibility of constructing a *quantitative* theory based on the random transfer matrix approach, which possesses a similar range of applicability.

For sufficiently long but finite segments, α_2 can be ignored and the random-phase result (2) yields a quantitative expression for α, provided of course that the resistances ρ_i are known. Unfortunately, because it is simpler to deal with asymptotic formulas, the problem of calculating the resistance ρ_i of a long but finite segment is much more difficult than the initial problem of determining the resistance of a system of length greater than $1/\alpha$. For this reason the random-phase assumption is not very useful in quantitative work.

In the present paper, we derive an exact recursion relation for the key phase (denoted ϵ in what follows) of the problem and show how it may be employed to yield a quantitative result for α in two limits. In Sec. IV, the large-ρ limit is discussed and an efficient numerical algorithm is described. In Sec. V, the small-ρ analysis is presented. The final results are rather general and for purposes of illustration, we apply them to a random sequence of delta functions. Throughout this paper the separations (rather than positions) of the delta functions are chosen to be random variables with mean y_0 and rectangular distribution of width $2\Delta y$. The lack of long-range order arising from the absence of an underlying crystal lattice has led to this system being regarded as a model of 1D liquid.[3] In a subsequent publication,[14] the results are applied to a

tight-binding Hamiltonian and the connection with a renormalization-group approach[15] to this problem is discussed.

Our aim is to derive simple quantitative formulas for the inverse localization length. These formulas may be obtained without a detailed knowledge of the behavior of the phase ϵ, because an average is taken over this phase to obtain the inverse localization length. Nevertheless, an explanation of the *properties* of α requires a deeper understanding. For this reason in Sec. III, we examine the recursion relation for ϵ in some detail. We demonstrate that in the limit of zero disorder the behavior of ϵ is intimately connected with the underlying band structure. Furthermore, it is noted that the recursion relation for ϵ possesses many of the features of the finite difference equations recently studied in theories of chaos.[16,17] In particular we show that ϵ possesses fixed points and chaotic regions. To begin with, however, in the next section we present a brief discussion of the formulation of the problem in terms of transfer matrices.

II. THE RANDOM T-MATRIX APPROACH

The electrical resistance $\mathscr{R}$ of a scattering system with a single input and a single output channel is given by[8]

$$\mathscr{R}=(h/2e^2)\frac{R}{T}\sim 13\frac{R}{T}\ \text{k}\Omega\ , \tag{3}$$

where T and $R=1-T$ are the transmission and reflection coefficients of the channel (a factor of 2 for spin has been included).

A one-dimensional potential can always be broken into a series of segments. In what follows, the dimensionless resistance R/T corresponding to a sequence of n segments will be denoted z_n. The requirement that at some stage in the analysis the dimensionless resistance ρ_i $(i=1,2,\ldots,n)$ of the individual segments must be calculated, leads one to adopt a simple choice for this subdivision. An example is given in Fig. 1, where each segment contains a single scatterer.

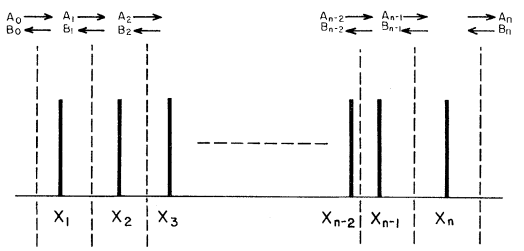

FIG. 1. A sequence of equal-strength delta functions with random separations. Each segment is defined to contain a single delta function.

The dimensionless resistance z_n is obtained after introducing transfer matrices. Consider a plane wave incident on a sequence of n scatterers as shown in Fig. 1. The transfer matrix $\overleftrightarrow{M}_n$ of the sequence is defined to yield the wave amplitudes to the right of the sequence, given the amplitudes on the left,

$$\begin{bmatrix} A_n \\ B_n \end{bmatrix}=\overleftrightarrow{M}_n\begin{bmatrix} A_0 \\ B_0 \end{bmatrix}\ . \tag{4}$$

A similar definition applies to the transfer matrix of a single scatterer. For the jth segment we write

$$\begin{bmatrix} A_{j+1} \\ B_{j+1} \end{bmatrix}=\overleftrightarrow{T}_j\begin{bmatrix} A_j \\ B_j \end{bmatrix}\ . \tag{5}$$

Comparing Eq. (4) with (5) yields the result

$$\overleftrightarrow{M}_n=\overleftrightarrow{T}_n\overleftrightarrow{T}_{n-1}\cdots\overleftrightarrow{T}_1\ , \tag{6}$$

which can be written more compactly in the form of a recursion relation

$$\overleftrightarrow{M}_n=\overleftrightarrow{T}_n\overleftrightarrow{M}_{n-1}\ . \tag{7}$$

The main reason why the following analysis can be applied to a wide range of 1D potentials is that the form of the transfer matrices is determined by symmetry arguments.[3,8] It is easy to show that time-reversal symmetry and current conservation require the following form for the transfer matrix $\overleftrightarrow{M}_n$,

$$\overleftrightarrow{M}_n=\begin{bmatrix} (1+z_n)^{1/2}e^{-i\mu_n} & z_n^{1/2}e^{-i\nu_n} \\ z_n^{1/2}e^{i\nu_n} & (1+z_n)^{1/2}e^{i\mu_n} \end{bmatrix}\ . \tag{8}$$

This expression involves the dimensionless resistance z_n and two phases μ_n and ν_n which depend on the detailed nature of the scattering system. The transfer matrix for the jth segment must have the similar form

$$\overleftrightarrow{T}_j=\begin{bmatrix} (1+\rho_j)^{1/2}e^{-i\theta_j} & \rho_j^{1/2}e^{-i\phi_j} \\ \rho_j^{1/2}e^{i\phi_j} & (1+\rho_j)^{1/2}e^{i\theta_j} \end{bmatrix} \tag{9}$$

which again involves two phases θ_j,ϕ_j and the dimensionless resistance ρ_j of the jth scatterer. In what follows, we assume that θ_j, ϕ_j, and ρ_j are known, so the problem of determining z_n and hence the inverse localization length α is reduced to that of solving Eq. (7).

Substituting Eqs. (8) and (9) into Eq. (7) yields after some simple algebra, the following recursion relations:

$$\ln(1+z_n)=\ln(1+z_{n-1})+\ln(1+\rho_n)+\ln(1+t_n^2+2t_n\cos\epsilon_n)\ , \tag{10}$$

$$r_n \exp[i(\epsilon_{n+1}-\delta_{n+1})]=\frac{s_n+r_{n-1}\exp(i\epsilon_n)}{1+s_n r_{n-1}\exp(i\epsilon_n)}\ , \tag{11}$$

where

$$\epsilon_n=\theta_n-\phi_n+\mu_{n-1}+\nu_{n-1}\ , \qquad \delta_n=\theta_n-\phi_n+\theta_{n-1}+\phi_{n-1}\ , \tag{12}$$

and

$$s_n=\left[\frac{\rho_n}{1+\rho_n}\right]^{1/2},\quad r_n=\left[\frac{z_n}{1+z_n}\right]^{1/2},$$

and

$$t_n=s_n r_{n-1}\ . \tag{13}$$

Equation (10) was originally obtained by Anderson *et al.*[8] using a slightly different method and demonstrates that ϵ is the relevant phase for a determination of z_n. Equation (11) is new and shows further that ϵ is a cumulative phase which can in general depend on all previous scatterers on the chain.

These equations are exact and completely general and we use them to obtain α in the limit $n\to\infty$. In this limit iterating Eq. (10) yields

$$\ln(1+z_n)=n\alpha=n(\alpha_1+\alpha_2)\ , \tag{14}$$

where

$$\alpha_1=\frac{1}{n}\sum_{i=1}^{n}\ln(1+\rho_i)\equiv\langle\ln(1+\rho)\rangle \tag{15}$$

and

$$\alpha_2=\frac{1}{n}\sum_{i=2}^{n}\ln(1+t_i^2+2t_i\cos\epsilon_i)\ . \tag{16}$$

A key feature of our approach is that the localized nature of the eigenstates of a 1D random system[18] can be used to simplify the formulas for α_2 and ϵ in the thermodynamic limit. We note that z_n increases with n, so for some $i\gg 1$ we can make the replacement $r_i=1$ in Eq. (16). In the limit $n\to\infty$, the finite number of terms corresponding to small i, for which this replacement is not permissible, have a negligible weight. Hence in this limit, Eq. (16) can be written

$$\alpha_2=\langle\ln(1+s^2+2s\cos\epsilon)\rangle\ . \tag{17}$$

Since $\{\rho_i\}$ are given, α_1 can immediately be calculated. On the other hand, until an expression is obtained for ϵ_i involving only "local" properties of individual segments, (17) cannot be evaluated. In the literature,[8–11] this problem has been avoided by introducing the assumption that ϵ is a random phase distributed uniformly over 2π. Note that for any s,

$$\frac{1}{2\pi}\int_0^{2\pi}d\epsilon\ln(1+s^2+2s\cos\epsilon)=0\ . \tag{18}$$

This "random-phase assumption" yields a vanishing result for α_2. As mentioned in the Introduction, this assumption is not generally valid. However, it is clear from (15) that by choosing long enough segments, ρ_i and hence α_1 can be made arbitrarily large. On the other hand, for finite disorder α_2 is *bounded* and hence the ratio α_2/α_1 can be made negligibly small. Unfortunately, since an expression for the dimensionless resistances ρ_i of long but finite segments is not available, this observation only yields the qualitative behavior of α.

To obtain quantitative results, we avoid the random-phase assumption and instead employ Eq. (11) to determine ϵ. The analysis for large and small ρ_i is presented in Secs. IV and V, respectively. However, before proceeding to this, it is useful to discuss some properties of the phase ϵ and in the following section we examine this quantity in the zero-disorder limit.

III. ENERGY BANDS AND THE PHASE ϵ

In this section we examine the phase ϵ in the zero-disorder limit and establish a connection between the behavior of this quantity and the band edges of the system. For simplicity our discussion will center on Borland's condition[19] for the band gaps of a sequence of equal-strength scatterers with random separations. This is given in (19) below and possesses two desirable features. First, the detailed nature of the scatterers need not be specified. Second, it is readily written in terms of the local phases δ_i of Eq. (12).

For a sequence of equal-strength scatterers we have for all i, $\rho_i=\rho$. Furthermore, the phases δ_i are in general distributed with some probability over the interval $(\delta_0-\Delta)$ to $(\delta_0+\Delta)$. In its original form,[19] Borland's condition was stated explicitly in terms of the minimum spacing between adjacent scatterers, the disorder in this spacing, and the incident electron energy. However, it is readily verified that in the notation of the present paper, Borland's condition can be restated as follows: When the following inequalities are satisfied, the incident electron energy lies within a band gap

$$\tan^{-1}\rho^{1/2}-\frac{\Delta}{2}+m\pi\geq\frac{\delta_0}{2}\geq m\pi-\tan^{-1}\rho^{1/2}+\frac{\Delta}{2}\ , \tag{19}$$

where m is an integer that can be used to label the gaps. The band structure obtained by examining the equalities of (19) is sketched in Fig. 2.

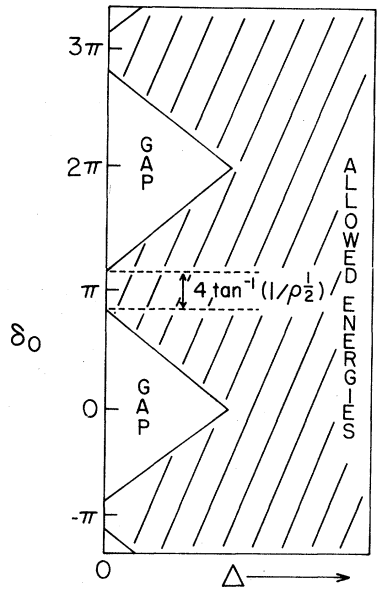

FIG. 2. A sketch of the band structure of a sequence of equal-strength scatterers with bounded disorder in the separations. For such a system, the phases δ_i are distributed over an interval $\delta_0-\Delta$ to $\delta_0+\Delta$, which in general depends on the incident electron energy and the scattering strengths. For a given ρ, this figure shows the pairs of values (δ_0,Δ) which correspond to allowed energies and to band gaps.

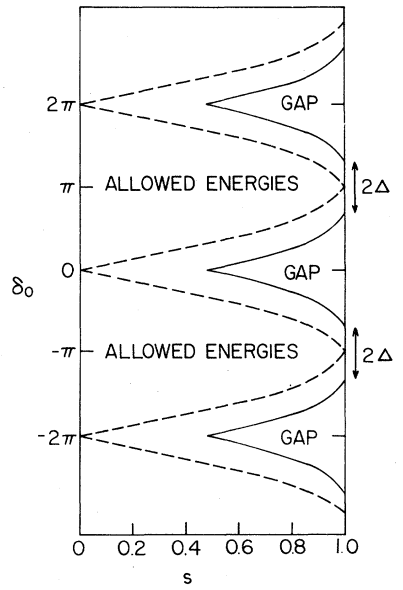

FIG. 3. For the sequence of scatterers used in Fig. 2, this figure shows the band structure as a function of the parameters δ_0 and $s=[\rho/(1+\rho)]^{1/2}$, for two values of the disorder Δ. The solid line shows the energy bands and gaps for $\Delta=1$ and the dashed curve for zero disorder $\Delta=0$.

At zero disorder (i.e., $\Delta=0$), the inequality (19) reduces to the condition

$$\tan^2(\delta_0/2)\leq\rho\ , \tag{20}$$

which is readily shown to be equivalent to the Kronig-Penney condition for the band edges.[20] For large disorder, the inequalities cannot be simultaneously satisfied and all the energy gaps disappear. This situation arises when

$$\Delta>2\tan^{-1}\rho^{1/2}\ .$$

More generally, Eq. (19) and Fig. 2 show that for a given value of ρ, there are pairs of values (δ_0,Δ) for which the incident electron energy corresponds to a gap in the density of states. At *zero disorder* the ranges of ρ_0 which correspond to allowed bands are of width

$$(2\pi-2\tan^{-1}\rho^{1/2})-(2\tan^{-1}\rho^{1/2})=4\tan^{-1}(1/\rho^{1/2})\ ,$$

while corresponding gap regions are of width $2\tan^{-1}\rho^{1/2}$.

It is also instructive to examine the band structure as a function of the parameter $s=[\rho/(1+\rho)]^{1/2}$ introduced in Eq. (13). For a disorder of $\Delta=1$, this is given by the solid curves of Fig. 3. It can be seen that for small s the band gaps have disappeared and all energies are allowed. The dashed curves show the corresponding band structure in the zero-disorder limit. At $s=0$ these show that the energy *gaps* are of infinitesimal width centered on values of δ_0 equal to integral multiples of 2π. Similarly at $s=1$ $(\rho=\infty)$ the energy *bands* are of vanishing width occurring at $\delta_0=(2n+1)\pi$, where n is some integer. For $\Delta=0$, the above values of δ_0 and s correspond to cusps in the dashed curve, and in what follows, it will be shown that to each cusp there is associated a singularity in the contribution α_2 to the inverse localization length.

Armed with the knowledge of the band structure, we now proceed to examine the behavior of the phase ϵ in the *zero-disorder limit.* In the thermodynamic limit where $r_n\to1$, Eq. (11) can be rewritten

$$\exp[i(\epsilon_{n+1}-\delta_{n+1})]=\frac{1+i\beta_n\left[\dfrac{\sin\epsilon_n}{1+\cos\epsilon_n}\right]}{1-i\beta_n\left[\dfrac{\sin\epsilon_n}{1+\cos\epsilon_n}\right]}=\exp\left\{2i\left[\tan^{-1}\left[\beta_n\tan\frac{\epsilon_n}{2}\right]\right]\right\}\ ,$$

where

$$\beta_n=\frac{1-s_n}{1+s_n} . \tag{21}$$

Hence

$$\tan\left[\frac{\epsilon_{n+1}-\delta_{n+1}}{2}\right]=\beta_n\tan\left[\frac{\epsilon_n}{2}\right] . \tag{22}$$

The complete asymptotic statistics of ϵ are contained in this formula.

To illustrate the behavior of ϵ, consider a sequence of equal-strength scatterers in which for all n, $\beta_n=\beta$. Consider also the limit of zero disorder where for all n, $\delta_n=\delta_0$. Then after writing

$$T_n=\tan\frac{\epsilon_n}{2} \quad \text{and} \quad t=\tan(\delta_0/2)$$

Eq. (22) becomes

$$T_{n+1}=(t+\beta T_n)/(1-\beta t T_n) . \tag{23}$$

We proceed by seeking a fixed point for this equation. Setting $T_{n+1}=T_n=T$ gives the result

$$T=\frac{1-\beta}{2\beta t}\left[1\pm\left[1-\frac{4\beta t^2}{(1-\beta)^2}\right]^{1/2}\right] , \tag{24}$$

which shows that for a given pair (β,t) there is a solution only if

$$t^2\le\frac{(1-\beta)^2}{4\beta} . \tag{25}$$

From (21) this can be written as

$$\tan^2(\delta_0/2)\le\rho . \tag{26}$$

Comparison with the inequality (20) reveals that (26) is simply the condition for δ_0 to correspond to a *band gap*. Hence, within a band in the zero-disorder limit Eq. (23) does *not* possess a fixed point.

The origin of this feature is revealed by using a flow diagram. Figure 4 shows the trajectory of $\epsilon/2$ arising from some initial value $\epsilon_1/2$. By expanding Eq. (23) about the fixed points (24) one can show that the fixed point corresponding to the plus sign in (24) is unstable, while the minus sign yields a stable fixed point. This can also be seen from Fig. 4 by constructing a few flows of the kind sketched. The origin of the condition (25) becomes evident when one seeks the maximum possible value of the difference

$$\delta/2=\epsilon/2-\tan^{-1}(\beta\tan\epsilon/2) .$$

The value of δ which yields this maximum is δ_{critical}, where

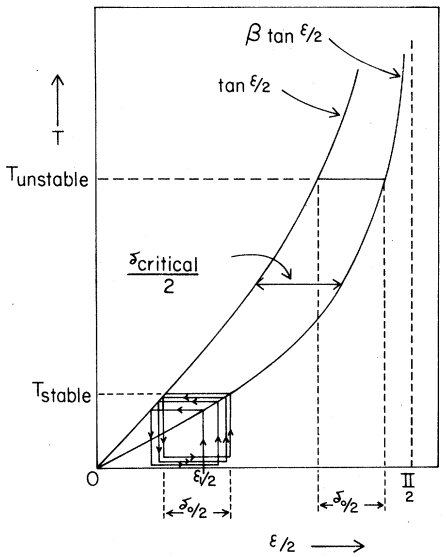

FIG. 4. A flow diagram for ϵ_n. Starting from some initial value ϵ_1 and with $\delta_0<\delta_{\text{critical}}$, the diagram shows how ϵ_n is "attracted" towards the stable fixed point.

$$\tan^2\left[\frac{\delta_{\text{critical}}}{2}\right]=\frac{(1-\beta)^2}{4\beta} . \tag{27}$$

These features are depicted in Fig. 4.

In view of (24) and (25), it is useful to introduce the parameter P given by

$$P^2=\frac{(1-\beta)^2}{4\beta t^2} . \tag{28}$$

The condition for δ_0 to correspond to a band of the zero-disorder system is then simply $P^2\le 1$. The fixed points as a function of P take the form of Fig.

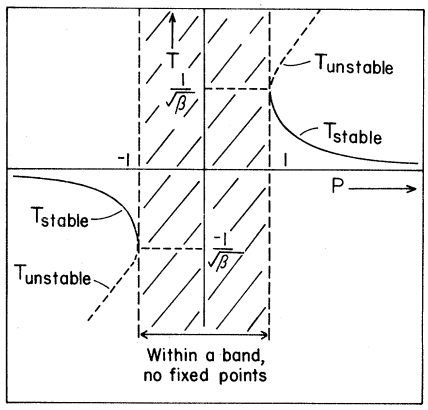

FIG. 5. A sketch of the fixed points as a function of the parameter P of Eq. (28). For $P<1$ there are no fixed points. For $P>1$ there is a stable and an unstable fixed point. These are $T_{\text{stable}}=P[1-(1-1/P^2)^{1/2}]/\beta^{1/2}$ and $T_{\text{unstable}}=P[1+(1-1/P^2)^{1/2}]/\beta^{1/2}$.

5. The behavior of the phase ϵ and its relationship to the zero-disorder band structure is illustrated by these two diagrams.

Equations (22) and (23) possess many of the features of the finite difference equations studied in the field of chaos.[16,17] Outside the region of stability the quantity T_n of Eq. (23) appears to exhibit chaotic behavior in certain regimes. Starting from two initial values T_1 and T_1' which are infinitesimally close together, we have found *numerically* that after a large number m of iterations, the corresponding quantities T_m and T_m' can be very far apart.

The approach to chaos (inside a band) from the stable behavior (outside the band) does not appear to follow any familiar route[17] (period doubling, intermittency, etc.). It may be that the weak-disorder limit corresponds to adding a noise term[21] to the finite difference equations for zero disorder. In view of these features, we feel that further exploration of the connection between localization and chaos should prove to be a fruitful subject of future research.

IV. THE LARGE-ρ LIMIT

We now proceed to obtain an expression for α_2 in the large-ρ limit. We note from Eqs. (21) and (13) that the quantity $\beta_n \leq 1$ and vanishes in the limit $\rho_n \to \infty$:

$$\beta_n = 1/4\rho_n + O(\rho_n^{-2}) . \tag{29}$$

Hence in view of Eq. (22), we consider replacing ϵ_{n+1} by δ_{n+1} in the large-ρ limit. This is reasonable provided the quantity $\epsilon_n/2$ on the right-hand side of (22) is not too close to $(n+\frac{1}{2})\pi$. More generally, for the purpose of computing the average on the right-hand side of Eq. (17), the replacement of ϵ by δ will yield a good approximation provided the probability is small that $\epsilon/2$ is close to $(n+\frac{1}{2})\pi$.

In the limit that for all i, $\rho_i \to \infty$, it can be shown that for any finite disorder Δ in the phases δ_i, the replacement

$$\epsilon_i = \delta_i \tag{30}$$

will yield an exact expression for α_2. Noting that

$$s_i = \left[\frac{\rho_i}{1+\rho_i}\right]^{1/2} = 1 + O(1/\rho) , \tag{31}$$

the resulting expression for α_2 from Eq. (17) is

$$\alpha_2 = \langle \ln(2+2\cos\delta) \rangle = \int d\delta\, P(\delta) \ln(2+2\cos\delta) , \tag{32}$$

where $P(\delta)$ is the distribution of the phases δ_i.

In the remainder of this section, we demonstrate the validity of Eq. (32) by examining a sequence of equal-strength delta functions with random separations. To calculate α_2 from (32), we need to know the transfer matrices $\overleftrightarrow{T}_i$ of individual segments introduced in Eq. (9). When each segment contains a simple delta function of strength ζ the well-known result[3] is

$$\rho^{1/2} = \frac{\zeta}{2k_0}, \quad \theta_j = \tan^{-1}\rho^{1/2} , \quad \phi_j = 2k_0 x_j + \pi/2 , \tag{33}$$

where k_0 is the wave vector of the incident electron and x_j the position of the jth delta function. Noting that

$$\tan^{-1}\rho^{1/2} = \pi/2 - 1/\rho^{1/2} + O(1/\rho)$$

yields from Eq. (12),

$$\delta_j = \pi - 2/\rho^{1/2} - 2k_0(x_j - x_{j-1}) + O(1/\rho) . \tag{34}$$

For simplicity we consider a model in which the *separations*

$$y_j = x_j - x_{j-1} \tag{35}$$

are uniformly distributed over the interval $y_0 \pm \Delta y$. In this case, the phases δ_j are uniformly distributed over the interval $\delta_0 \pm \Delta$, where

$$\delta_0 = \pi - 2/\rho^{1/2} - 2k_0 y_0 + O(1/\rho) \tag{36}$$

and

$$\Delta = 2k_0 \Delta y . \tag{37}$$

Hence Eq. (37) becomes

$$\alpha_2 = \frac{1}{2\Delta} \int_{\delta_0-\Delta}^{\delta_0+\Delta} d\delta \ln(2+2\cos\delta) . \tag{38}$$

From Eqs. (37) and (18) the random-phase result $\alpha_2 = 0$ will arise in the special case when $\Delta = \pi$ or $y = \pi/2k_0$. The result (38) has been given previously in a short Communication.[12]

We shall compare the value of α_2 predicted by (38) with the results of a *numerical simulation.* The latter may be carried out quite generally by generating the elements of the matrices $\overleftrightarrow{T}_j$ from the known properties of the single scatterers and their positions x_j. For delta functions this prescription is given by Eq. (33) and for the distribution mentioned above, the position x_{j+1} is obtained by adding a random number y_{j+1} to the position x_j. z_n can now be obtained by iterating both Eqs. (10) and (11). One advantage of a simulation based on Eqs. (10) and (11) is that exponentially large numbers associated with z_n are easily avoided. Equation (11) involves z_n only through the quantity r_n and as $z_n \to \infty$, $r_n \to 1$.

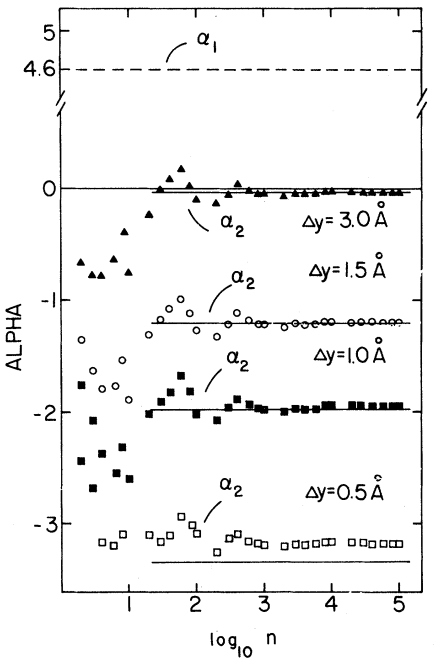

FIG. 6. Comparison of the analytic result (38) for α_2, shown by the solid line, with the results of a numerical simulation on a sequence of 10^5 equal-strength scatterers. The parameters used are $\rho=105$, $k_0=0.5123$ Å^{-1}, and $y_0=5.9424$ Å. The value of δ_0 given by Eq. (36) is $-\pi$ corresponding to the band center.

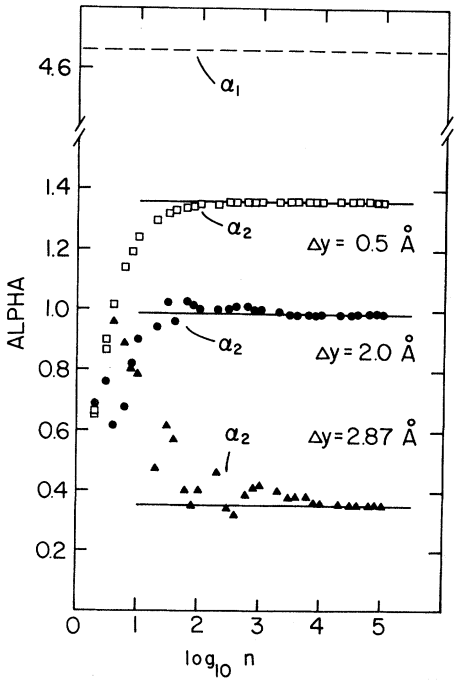

FIG. 7. Same as for Fig. 6 except that $y_0=2.876$ Å so that $\delta_0=0$, corresponding to the center of a band gap.

Hence as z_n becomes large one can replace r_n by unity and proceed with the iteration of Eq. (11). Furthermore, Eq. (10) only involves the logarithm of z_n and consequently the algorithm is numerically very stable. In practice the replacement of r_n by unity in Eq. (11) was carried out whenever z_n exceeded 10^{14}. For large ρ, since the localization length is small, this occurs after only a few iterations. However, for small ρ, where the localization length is large, greater distances are required. Nevertheless, for any finite disorder and in the thermodynamic limit $n\to\infty$, we found that in all cases $z_n\to\infty$ justifying our asymptotic solution (17) for α_2.

For an electron energy of 1 eV ($k_0=0.5123$ Å^{-1}), Fig. 6 shows the results of a simulation on a chain of 10^5 scatterers, each of dimensionless resistance $\rho=105$. The figure shows the variation of the contributions α_1 and α_2 with the size of the system n. The contribution α_1 is given by the dotted line and for equal-strength scatterers is simply a constant [see Eq. (15)]. The variation of α_2 with n is shown for three different values of disorder in the separations y_i, with corresponding disorder in δ given by Eqs. (36) and (37). The solid lines show the values of α_2 predicted by Eq. (38). For large n it can be seen that the numerical results settle down to the ex-

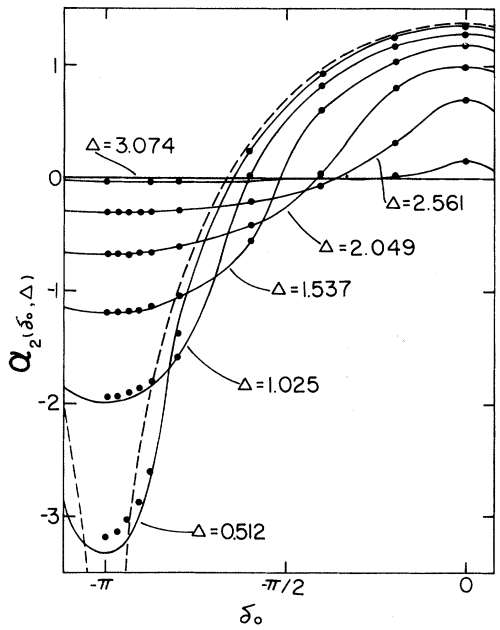

FIG. 8. For six different values of the disorder Δ the curves show the variation of $\alpha_2(\delta_0,\Delta)$ with the mean δ_0 [Eq. (39)]. The points give the corresponding asymptotic values of α_2 obtained from numerical simulations on sequences of 10^5 scatterers. The results for α_2 are periodic in 2π and even about the origin. The limiting case of $\Delta=0$ is shown by dashed lines.

pected asymptotic value.

For large disorder Δy, the quantity α_2 is very small reflecting the random-phase result. However, as the disorder decreases α_2 becomes increasingly negative and at $y=0.5$ Å, α_2 is almost the negative of α_1. For the results shown in Fig. 6, $y_0=5.942$ Å and setting $\Delta=0$ in Borland's condition[19] it is readily verified that the corresponding value of δ_0 falls precisely at the band center of the ordered solid. Hence the behavior of α_2 as the disorder decreases reflects the fact that the sum $\alpha=\alpha_1+\alpha_2$ must vanish within a band in the crystal limit. At the lowest value of the disorder shown in Fig. 6, there is a small discrepancy between the numerical results and the predicted asymptotic value. This is approaching a pathological limit as the bands become very flat in the large-ρ, zero-disorder limit. It is only in this limit that our result for large ρ [Eq. (32)] fails, as can be seen from Figs. 6–8. At this point α_2 is highly singular, since it must cancel the $\ln\rho$ divergence in α_1 to give $\alpha=0$ in the zero-disorder limit. Outside of the point bands, $\alpha\neq 0$ in the zero-disorder limit and the result (32) for α_2 is valid.

The behavior in Fig. 6 is in marked contrast with the results shown in Fig. 7. In this simulation the value of y_0 is chosen to be 2.876 Å, so the electron energy of 1 eV corresponds to the center of a gap ($\delta_0=0$). Again it can be seen that the numerical results settle down to the asymptotic value predicted by Eq. (38). For a disorder Δ approaching π, the random-phase result is obtained. However, as the disorder decreases, α_2 increases. From Eq. (38) it is clear that $-\infty<\alpha_2\leq\ln 4$.

For comparison of Eq. (38) with further numerical results, it is convenient to define the quantity

$$\alpha_2(\delta_0,\Delta)=\frac{1}{2\Delta}\int_{\delta_0-\Delta}^{\delta_0+\Delta} d\delta\,\ln(2+2\cos\delta) \qquad (39)$$

which can be evaluated by numerical integration. Figure 8 shows plots of $\alpha_2(\delta_0,\Delta)$ vs δ_0 for six different values of the disorder Δ. Superposed on these curves are the asymptotic values of α_2 obtained from various numerical simulations on the system of scatterers employed in Figs. 6 and 7. The quantity δ_0 was varied by adjusting the average spacing y_0 in Eq. (36). For all but the pathological limit of small Δ and δ_0 close to π (i.e., within a band at small disorder) the results are in excellent agreement. This agreement would be further improved using larger values of ρ.

Figures 6–8 illustrate that the behavior of α_2 is strongly affected by the underlying band structure. This becomes more evident when one examines plots of $\alpha_2(\delta_0,\Delta)$ vs Δ for various values of the mean δ_0. These are shown in Fig. 8. For any finite Δ, Eq. (32) is exact in the limit $\rho\to\infty$. In this limit Borland's condition (19) yields for the positions of the band edges

$$\delta_0=(2m+1)\pi\pm\Delta\ . \qquad (40)$$

These are given by the dashed curve in Fig. 9.

An interesting feature revealed by Fig. 9 is that increasing the disorder does not necessarily increase the resistance of the wire. For example, consider the curve corresponding to $\delta_0=2.827$. Starting from Δ close to zero, α_2 (and hence $\alpha=\alpha_1+\alpha_2$) decreases within the band as Δ increases until at some value of Δ just outside the band edge, corresponding to the minimum of the curve, α_2 begins to increase with Δ.

Also striking is the fact that these minima do *not* correspond to the band edges. By differentiating Eq. (39) with respect to Δ, we find a logarithmic singularity in $\partial\alpha_2/\partial\Delta$ at the *band edges* given by Eq. (40). This weak singularity shows up best in Fig. 9 for $\delta_0=2.827$. However, for finite ρ, it is unlikely that this divergence is present in the exact asymptotic expression for α_2 given in Eq. (17).

V. THE SMALL-ρ ANALYSIS

Having obtained an expression for α_2 in the large-ρ limit, we now proceed to analyze the problem in the limit of small ρ. In this limit $\beta\to 1$ and the analysis of the preceding section, which stems

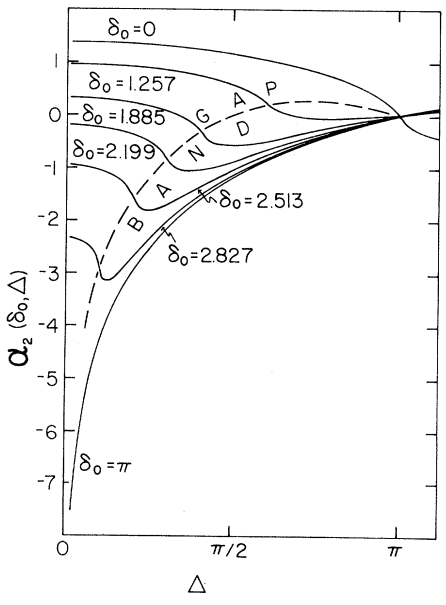

FIG. 9. For seven different values of the mean δ_0 the curves show the variation of $\alpha_2(\delta_0,\Delta)$ with disorder Δ obtained from Eq. (3). A pair of values (δ_0,Δ) corresponding to the intersection of the dashed line and a particular curve gives the position of the band edge.

from the replacement (30), is inappropriate. For small ρ we calculate α_2 without explicitly solving for ϵ. An extension of this analysis will be presented in a subsequent publication.[14] For clarity this initial analysis will be restricted to a sequence of equal-strength scatterers in which the separations are uncorrelated random variables.

We begin by series expanding the right-hand side of Eq. (17) in powers of the small parameter $s=[\rho/(1+\rho)]^{1/2}$. From (17)

$$\exp(i\epsilon_{n+1})=\exp(i\delta_{n+1})\exp(i\epsilon_n)+s\exp(i\delta_{n+1})\frac{[1-\exp(2i\epsilon_n)]}{[1+s\exp(i\epsilon_n)]} . \tag{42}$$

From Eq. (42), it can be shown by induction that for any finite disorder,

$$\langle\exp(mi\epsilon)\rangle=O(s^m) . \tag{43}$$

Hence contributions to α_2 neglected by retaining only the terms shown explicitly in Eq. (41) are $O(s^6)$.

Note that δ_{n+1} is linear in the separation y_{n+1} of the nth and $(n+1)$th scatterers. In particular for delta functions, Eqs. (33) and (12) yield

$$\delta_{n+1}=2\tan^{-1}\rho^{1/2}-2k_0y_{n+1} . \tag{44}$$

Therefore, δ_{n+1} is a random variable uncorrelated with ϵ_n, because the latter depends only on the first n scatterers while the former involves only the $(n+1)$th. We may write for any n and m,

$$\langle\exp(mi\epsilon_{n+1})\rangle=\langle\exp(mi\epsilon_n)\rangle=\langle\exp(mi\epsilon)\rangle$$

so averaging both sides of Eq. (42) yields the result

$$\langle\exp(i\epsilon)\rangle=\frac{s\langle\exp(i\delta)\rangle}{1-\langle\exp(i\delta)\rangle}\left\langle\frac{1-\exp(2i\epsilon)}{1+s\exp(i\epsilon)}\right\rangle . \tag{45}$$

It is convenient to introduce the notation

$$a_m=\langle\exp(mi\delta)\rangle . \tag{46}$$

Then in view of (43), expanding the right-hand side of Eq. (45) yields

$$\langle\exp(i\epsilon)\rangle=\frac{sa_1}{1-a_1}[1-\langle\exp(2i\epsilon)\rangle-s\langle\exp(i\epsilon)\rangle+O(s^4)] . \tag{47}$$

Similarly after squaring and averaging Eq. (42), one obtains

$$\alpha_2=\langle\ln[1+s\exp(i\epsilon)][1+s\exp(-i\epsilon)]\rangle=2\,\mathrm{Re}\{\langle\ln[1+s\exp(i\epsilon)]\rangle\}=\mathrm{Re}[2s\langle\exp(i\epsilon)\rangle-s^2\langle\exp(2i\epsilon)\rangle+\cdots] . \tag{41}$$

To obtain an expression for the averages on the right-hand side of this equation we set $r_n=1$ and write Eq. (11) in the form

$$\langle\exp(2i\epsilon)\rangle=\frac{sa_2}{1-a_2}[2\langle\exp(i\epsilon)\rangle+s+O(s^3)] . \tag{48}$$

Equation (45) shows that (43) is valid for $m=1$. Substituting Eq. (47) into Eq. (48) yields Eq. (43) with $m=2$ and as stated earlier the general proof follows by induction.

Equations (47) and (48) can now be solved for the averages on the right-hand side of Eq. (41) to yield the result

$$\alpha_2=b_1s^2+b_2s^4+O(s^6) , \tag{49}$$

where

$$b_1=\mathrm{Re}\left[\frac{2a_1}{1-a_1}\right] \tag{50}$$

and

$$b_2=\mathrm{Re}\left[\frac{\alpha_2(1-a_1^2)+2a_1(a_1+a_2)}{(1-a_1)^2(a_2-1)}\right] . \tag{51}$$

Equations (49)–(51) apply to any system of equal-strength scatterers in which δ_{n+1} is a random variable uncorrelated with the previous δ_n. This is true for the model of a disordered "liquid" used to illustrate the results of the preceding section. Before comparing Eqs. (49)–(51) with the results of a corresponding numerical simulation in the small-ρ limit, it is appropriate to remark on the range of validity of these equations. Equation (41) suggests that for finite disorder and small enough ρ, α_2 is an analytic function of s. A similar remark holds for the averages $\langle\exp(mi\epsilon)\rangle$. Hence in principle by computing higher-order coefficients the present analysis could be extended into the large-ρ regime.

In the limit of zero disorder, all quantities a_m are of modulus unity leading to divergencies. Consider for example Eq. (45), which is an exact expression for $\langle\exp(i\epsilon)\rangle$. Since the modulus of this quantity cannot exceed unity, it is clear that a vanishing of

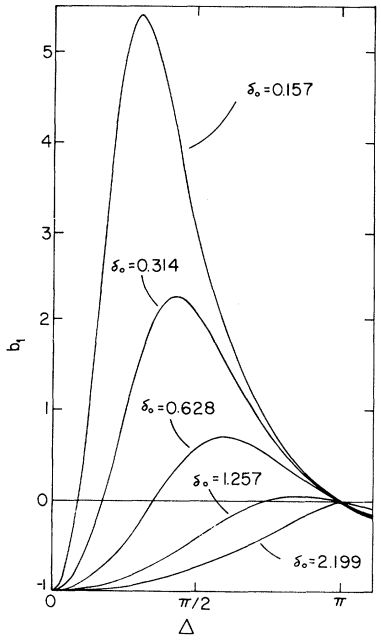

FIG. 10. Variation of the coefficient b_1 of Eq. (55) as a function of the disorder Δ.

the denominator $(1-a_1)$ will be accompanied by a zero result for the expectation value on the right-hand side. However, in view of Eq. (48) we obtain from Eq. (45)

$$\frac{\partial}{\partial s}\langle \exp(i\epsilon)\rangle\Big|_{s=0} = \frac{a_1}{1-a_1} . \tag{52}$$

Furthermore, Eq. (41) yields

$$\frac{\partial}{\partial(s^2)}\alpha_2\Big|_{s=0} 2 = \frac{\partial}{\partial s}\langle \exp(i\epsilon)\rangle\Big|_{s=0} \tag{53}$$

so that Eq. (52) demonstrates that in the limit $s\to 0$ the first derivative of α_2 with respect to s^2 possesses a simple pole at $a_1=1$. If s is not too large, the first two terms of (49) yield a good approximation to α_2, provided this singularity is avoided.

To illustrate these features we now apply Eqs. (49)—(51) to the situation in which the phases δ_i are uniformly distributed over the interval $\delta_0\pm\Delta$. In this case

$$a_m = e^{im\delta_0}\,\frac{\sin m\Delta}{m\Delta} \tag{54}$$

and Eq. (50) yields

$$b_1 = s\frac{\sin\Delta}{\Delta}\left[\frac{\cos\delta_0 - \dfrac{\sin\Delta}{\Delta}}{1-2\dfrac{\sin\Delta}{\Delta}\cos\delta_0+\left[\dfrac{\sin\Delta}{\Delta}\right]^2}\right] . \tag{55}$$

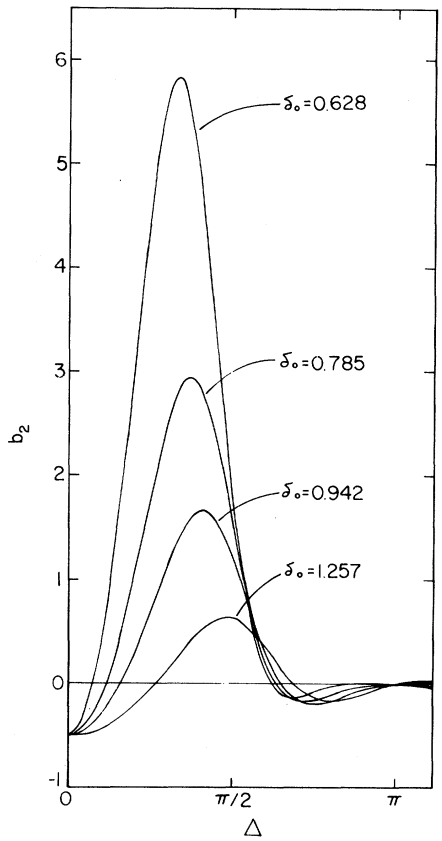

FIG. 11. Variation of the coefficient b_2 of Eq. (49), obtained after substituting Eq. (54) into Eq. (51), as a function of the disorder Δ.

The expression for b_2 is more cumbersome and for brevity will be omitted. For various values of δ_0, the variation with Δ of the coefficients b_1 and b_2 is shown in Figs. 10 and 11, respectively. A common feature of these curves is the presence of a maximum that increases in magnitude and shifts towards $\Delta=0$ as δ_0 decreases towards zero. This reflects the divergence in the derivatives of α_2 at $a_1=1$.

We now employ Eq. (55) and the corresponding expression for b_2 to compare (49) with the results of a numerical simulation on a sequence of 10^6 equal-strength delta functions with $\rho=0.065$. Figure 12 shows the results for a value of δ_0 equal to $-\pi$, corresponding precisely to the center of a band. The solid lines show the asymptotic values of α_2 predicted by Eq. (49) and are in excellent agreement with the numerical results. In common with the large-ρ, in-band behavior, α_2 becomes increasingly negative as the disorder decreases and cancels with α_1 in the limit $\Delta\to 0$. This is typical of the behavior of α_2 for almost all energies, because in the small-ρ limit, band gaps are either nonexistent or extremely narrow.

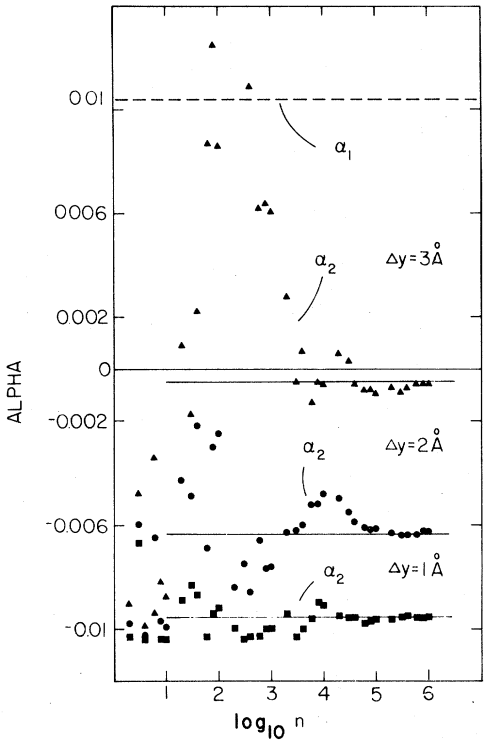

FIG. 12. Comparison of the analytic result (49) for α_2, shown by the solid line, with the results of a numerical simulation on a sequence of 10^6 equal-strength scatterers. The parameters used are $\rho=0.065$, $k_0=0.5123$ Å^{-1}, and $y_0=3.265$ Å. The value of δ_0 is $-\pi$ corresponding to a band center.

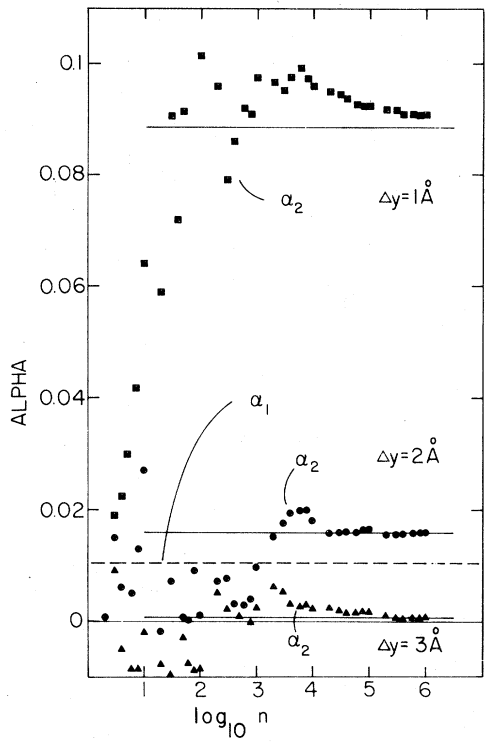

FIG. 13. Same as for Fig. 12 except that $y_0=3.63$ Å so that $\delta_0=0$, corresponding to the center of a gap.

Figure 13 shows the results of a numerical simulation in which $\delta_0=0$. This corresponds to the center of an energy gap of the ordered system (see Figs. 2 and 3) and in the limit $\Delta\to 0$ falls precisely on the divergence which occurs when $a_1=1$. Nevertheless, except at the smallest values of Δ, Eq. (49) yields the correct result for the asymptotic value of α_2. Other than in the region close to the pole (i.e., δ_0 and Δ close to zero) the contribution to α_2 from the second term on the right-hand side of (49) was found to be negligible. In the vicinity of the pole (e.g., for the $\Delta y=1$ Å results of Fig. 13) the contribution from this term is significant.

VI. DISCUSSION

In this paper we have derived formulas for the inverse localization length of a 1D random potential. The general arguments leading to these expressions did not make use of the detailed nature of the scatterers. As a result, the method can be used to study any 1D potential that can be conveniently divided into segments. With modifications it can also be applied to tight-binding Hamiltonians[14] where some analytic results are already known.[6,7] Throughout this work we have avoided averaging over ensembles of equivalent chains. Instead, we made use of the fact that in the thermodynamic limit, the physically relevant quantity α is *self-averaging.*

To illustrate the general results, a sequence of equal-strength, randomly spaced delta functions was considered. The analytic expressions were compared with the results of a numerical simulation on chains of up to 10^6 scatterers. The numerical algorithm is rather efficient and for 10^6 scatterers takes only about 100 sec of computer time on a CDC Cyber 750. Except near isolated singularities associated with the band centers in the strong-scattering limit and the gap centers in the weak-scattering limit, the results were in good agreement.

The new analytic expressions derived in this paper are extremely useful for obtaining an overall understanding of the problem. As a result of this work, we have shown that the random-phase assumption of $\alpha_2=0$ is unreliable in yielding quantitative results unless the phase is randomized at each scattering event. Choosing larger segments, containing many scatterers, does lead eventually to $\alpha_2'=0$ where the prime refers to the longer segments. However, this is *not* because the random-phase assumption becomes valid but merely because the original problem

of a long chain is being solved and α_2' becomes a surface or end effect.[12]

We have found an interesting connection with recent work on *chaos*. This is not surprising as the key phase of the problem ϵ is determined from a set of finite difference equations. In the zero-disorder limit, we found that the phase ϵ has a single stable fixed point in the band-gap region and appears to behave chaotically inside the energy bands. This will be discussed in a subsequent paper.[22]

Although all the work in this paper has been confined to 1D, some of it may have an impact on current thinking in higher dimensions. In particular, the random-phase assumption has been used in higher dimensions to obtain scaling relations. We believe this needs further consideration particularly in the borderline case of two dimensions.

ACKNOWLEDGMENTS

We should like to thank P. Erdös for a useful conversation. This work was supported in part by the National Science Foundation.

[1]For an early review see D. J. Thouless, Phys. Rep. 13C, 93 (1974).
[2]N. Giordano, W. Gilson, and D. E. Prober, Phys. Rev. Lett. 43, 725 (1979).
[3]P. Erdös and R. C. Henderson, Adv. Phys. 31, 65 (1982).
[4]J. Sak and B. Kramer, Phys. Rev. B 24, 1761 (1981).
[5]B. Andereck and E. Abrahams, J. Phys. C 13, L383 (1980).
[6]D. Sarker, Phys. Rev. B 25, 4304 (1982).
[7]A. D. Stone and J. D. Joannopoulos, Phys. Rev. B 24, 1761 (1981).
[8]P. W. Anderson, D. J. Thouless, E. Abrahams, and D. S. Fisher, Phys. Rev. B 22, 3519 (1980); E. Abrahams and M. Stephen, J. Phys. C 13, L377 (1980).
[9]P. W. Anderson, Phys. Rev. B 23, 4828 (1981).
[10]R. Landauer, Philos. Mag. 21, 863 (1970).
[11]E. Abrahams and M. Stephen, J. Phys. C 13, L377 (1980).
[12]C. J. Lambert and M. F. Thorpe, Phys. Rev. B 26, 4742 (1982).
[13]It is to be noted that this is *not* because the phases randomize as the segment length increases. It is simply that by choosing longer segments, weight can be shifted from α_2 to α_1.
[14]C. J. Lambert, J Phys. C (in press).
[15]C. J. Lambert, Phys. Lett. 78A, 471 (1980).
[16]See, for example, R. M. May, Nature 261, 459 (1976); R. M. May and G. F. Oster, Am. Nat. 110, 573 (1976).
[17]For a recent review see D. J. Scalapino, J. E. Hirsch, and B. A. Huberman in *Melting, Localization and Chaos,* edited by R. K. Kalia and P. Vashishta (North-Holland, Amsterdam, 1982), p. 243.
[18]H. Furstenberg, Trans. Am. Math. Soc. 1-8, 377 (1963).
[19]R. E. Borland, Proc. Phys. Soc., London 77, 705 (1961).
[20]R. de L. Kronnig and W. G. Penney, Proc. R. Soc., London Sect. A 130, 499 (1931).
[21]J. P. Crutchfield and B. A. Huberman, Phys. Lett. 77A, 407 (1980).
[22]C. J. Lambert, P. Beale, and M. F. Thorpe (unpublished).